The Effect of Tropospheric Fluctuations on the Accuracy of Water Vapor Radiometry

J. Z. Wilcox
Tracking Systems and Applications Section

Line-of-sight path delay calibration accuracies of 1 mm are needed to improve both angular and Doppler tracking capabilities. Fluctuations in the refractivity of tropospheric water vapor limit the present accuracies to about 1 nrad for the angular position and to a delay rate of 3×10^{-13} sec/sec over a 100-sec time interval for Doppler tracking. This article describes progress in evaluating the limitations of the technique of water vapor radiometry at the 1-mm level. The two effects evaluated here are: (1) errors arising from tip-curve calibration of WVR's in the presence of tropospheric fluctuations and (2) errors due to the use of nonzero beamwidths for water vapor radiometer (WVR) horns. The error caused by tropospheric water vapor fluctuations during instrument calibration from a single tip curve is 0.26 percent in the estimated gain for a tip-curve duration of several minutes or less. This gain error causes a 3-mm bias and a 1-mm scale factor error in the estimated path delay at a 10-deg elevation per 1 g/cm^2 of zenith water vapor column density present in the troposphere during the astrometric observation. The error caused by WVR beam averaging of tropospheric fluctuations is 3 mm at a 10-deg elevation per 1 g/cm^2 of zenith water vapor (and is proportionally higher for higher water vapor content) for current WVR beamwidths (full width at half maximum of approximately 6 deg). This is a stochastic error (which cannot be calibrated) and which can be reduced to about half of its instantaneous value by time averaging the radio signal over several minutes. The results presented here suggest two improvements to WVR design: First, the gain of the instruments should be stabilized to 4 parts in 10^4 over a calibration period lasting 5 hours, and second, the WVR antenna beamwidth should be reduced to about 0.2 deg. This will reduce the error induced by water vapor fluctuations in the estimated path delays to less than 1 mm for the elevation range from zenith to 6 deg for most observation weather conditions.

I. Introduction

Future missions will benefit from spacecraft tracking with 100-prad accuracy in an angular position. The Cassini radio science team requires a delay-rate accuracy of 5×10^{-16} sec/sec over 1000 sec for gravitational wave searches using Doppler tracking. Fluctuations in wet tropospheric refractivity limit the present tracking capabilities to about 1 nrad for angular position and 5×10^{-14} sec/sec over 1000 sec for Doppler tracking, which corresponds to a 0.1-mm/sec uncertainty in spacecraft radial velocity.

Angular tracking is done with very long baseline interferometry (VLBI), a technique that measures the differential phase between two DSN antennas of an electromagnetic signal originating from a radio source. By relating this measured phase difference to geometrical path delays, astrometric parameters can be estimated. Inhomogeneities in tropospheric refractivity cause unmodeled errors in the path delay at about the 1-cm level for a path delay at zenith over a period of several hours. This error corrupts angular position estimates at about the 1-nrad level. To achieve 100-prad angular position accuracy, fluctuations in path delays must be calibrated at the 1-mm level [1,2].

Charged particles (both in the Earth's ionosphere and in solar wind) are the main source of error for spacecraft gravitational wave searches using Doppler tracking at S-band (2.3 GHz) (all missions prior to Galileo). Searches planned for Galileo at X-band (8.4 GHz) will be limited by fluctuations in the plasma and the troposphere at about the same level, a delay rate of approximately 5×10^{-15} sec/sec over 1000 sec [3]. In searches planned for Cassini at K-band (32 GHz), the increased observational frequency will reduce the plasma-induced error to approximately 5×10^{-16} sec/sec over 1000 sec. To take advantage of this increased sensitivity, tropospheric fluctuations must be calibrated at the submillimeter level.

Water vapor radiometers (WVR's) have been suggested for measuring line-of-sight path delays due to tropospheric water vapor. WVR's work on the principle that the radio power collected by a WVR antenna is proportional to the brightness temperature of the sky in the antenna pointing direction. Path-delay retrieval algorithms relate the brightness temperatures measured at two (or more) frequencies near the 22.6-GHz water vapor absorption line to a path delay associated with tropospheric water vapor along a line of sight in the same direction [4]. Brightness temperatures at two or more frequencies are required to subtract the effect of liquid water absorption from the total absorption. Unlike water vapor, liquid water does not affect the refractivity at microwave frequencies.

The ability of WVR's to determine the absolute path delays, or to track path delay changes induced by tropospheric fluctuations, has been tested recently with mixed results.[1–3] The accuracy of WVR calibration using radiosondes is limited at a level of approximately 10 percent (which causes a 0.6-cm error for a 6-cm zenith path delay) due to uncertainties in both the radiosonde data and path delay retrieval algorithms [4].[2] Studies that calibrated VLBI time series with differenced WVR delays using copointed antennas reported reduced rms residual delays at high elevations,[3] but the residual delays actually increased (up to 20 psec, corresponding to a 0.6-cm path delay error) at elevations below 50 deg. These results strongly suggest that to meet the future mission requirements, the character of various error sources that affect the accuracy of water vapor radiometry must be much better understood.

The accuracy with which WVR's estimate tropospheric path delays is determined by error sources that include (but are not restricted to) inaccuracies in calibration of the WVR gain, uncertainties in the path-delay retrieval algorithms and atmospheric absorption modeling, radiometer noise, the effect of the WVR location relative to the radio telescope, and the beam intensity distribution. The error sources will be discussed later. The errors can originate in the instrument or in the atmosphere and can cause bias, scale, or random errors in the retrieved path delays. The effect of a constant bias on path delays for angular tracking can be eliminated by differencing between observations. Biases have no effect on delay rates used for gravitational wave searches. Unmodeled variability in spatial distributions of atmospheric parameters together with the system noise have been recognized as the principal noise mechanisms that limit the ability of WVR's to monitor tropospheric fluctuations. Only recently has it been recognized that for any realistic WVR design, the tropospheric dynamics will also influence the WVR accuracy.

[1] T. J. Vesperini, "Staplelon WVR Experiment–Part I: Results," JPL Interoffice Memorandum (internal document), Jet Propulsion Laboratory, Pasadena, California, March 7, 1988.

[2] S. Keihm, "Water Vapor Radiometer Intercomparison Experiment: Platteville, Colorado, March 1–14, 1991," *Final report, JPL Task Plan 80-3289* (internal document), Jet Propulsion Laboratory, Pasadena, California, July 1991.

[3] C. Edwards, "Water Vapor Radiometer Line-of-Sight Calibration Capabilities," JPL Interoffice Memorandum 335.1-90-015 (internal document), Jet Propulsion Laboratory, Pasadena, California, March 30, 1990.

The main goal of this article is to investigate how the tropospheric dynamics affect the WVR's ability to track tropospheric fluctuations. Because WVR's are imperfect instruments, one of the goals of this article is to quantify relations between WVR design parameters and path-delay retrieval accuracy. To understand how the errors affect path delay estimates, an analysis of the effect of WVR error sources on path delay retrieval is presented. The article then focuses on two specific errors that arise from tropospheric fluctuations: errors in WVR instrument gain calibration from tip curves and errors caused by WVR antenna beam averaging. Tropospheric fluctuations cause errors in the estimated gain because data at different tip directions are analyzed using mapping relationships valid for a temporally constant and spatially homogeneous troposphere. Tropospheric fluctuations cause unmodeled departures from this picture, which induces errors in the estimated gain and ultimately in the estimated path delays. WVR antenna beam averaging causes errors in the estimated brightness temperature in the direction of a radio telescope because data recorded by the WVR's are beam averaged around the WVR pointing direction (full beam widths of the present state-of-the-art WVR's are between 4 and 10 deg), whereas radio telescopes measure the tropospheric effects along the line of sight to a distant radio source. The averaging corrupts the accuracy of the estimated brightness temperature in the radio source direction for all realistic WVR designs.

The article is organized as follows: Section II discusses how various error sources affect path delay estimates. Some basic equations describing the conversion of the recorded data to the line-of-sight path delay are given. Section III calculates the error in the WVR measurement incurred by using tip curves in an inhomogeneous troposphere. This error will exist as long as the WVR's are calibrated by using tip curves. Section IV studies the effect of beam averaging on WVR measurements for collocated antennas. The effects of antenna copointing and beam intensity distribution are discussed. The aim here was not to derive exact numbers for any specific WVR design but rather to provide rough error estimates. Section V is a summary with recommendations for WVR gain stability requirements and antenna beam width design to comply with the 1-mm path-delay accuracy requirement, as well as plans for further studies.

II. WVR Error Sources and Their Effect on Path Delay Retrieval

To put the above-mentioned effects in perspective, this section gives an overview of how various error sources affect the estimated path delay. The conclusions of this overview are summarized in Fig. 1. Error sources result from inaccuracies in WVR measurements or data interpretation and can cause bias, scale, or random effects in the retrieved path delay. The effect of a constant bias or linear trend on the tracking of changes in the path delay can be eliminated with astrometric parameter estimation. A scale error is an error that is directly proportional to the path delay. It is unclear at the present time to what extent radiometric data reduction can filter out the effect of a systematic scale error on astrometric parameter estimates. Stochastic errors cannot be reduced by parameter estimation. The effect of error sources on the estimated path delays can be analyzed by using a path delay retrieval algorithm that relates the line-of-sight path delay (L_v) due to water vapor in the troposphere to the brightness temperature (T_B) in the same direction. For example, Eq. (20) of [4],

$$L_v = a_0 + a_1 T_{B,1} + a_2 T_{B,2} \tag{1}$$

expresses L_v as a linear combination of the brightness temperatures $T_{B,j}$ (j = 1,2) at frequencies f_1 = 20.6 GHz and f_2 = 31.4 GHz. In Eq. (1), a_j's are coefficients that have been determined by a regression analysis of the WVR data [4]. The value of a_0 quantifies the effect of the dry component of the atmospheric absorption; a_1 quantifies the effect of water vapor absorption; and the term $a_2 T_{B,2}$ ($a_2 \simeq -a_1 (f_1/f_2)^2$) subtracts the contribution due to tropospheric liquid water from the total absorption (liquid water causes a negligible path delay). For L_v in centimeters and $T_{B,j}$ in kelvins, typical regression coefficients are $a_0 \simeq -1.6$, $a_1 \simeq 0.66$, and $a_2 \simeq -0.3$. Typical $T_{B,j}$'s are between 10 and 100 K. The value of L_v scales as $L_v(\text{cm}) \simeq 6\ N_v / \sin E$, where N_v is the water vapor column density (in g/cm^2) at zenith, and E is the observed elevation. For typical N_v between 1 g/cm^2 and 4 g/cm^2, the zenith path delay ($L_{v,z}$) is between 6 and 24 cm.

Taking the differential of Eq. (1) determines the error in the retrieved path delay, δL_v, in terms of errors in the regression coefficients, δa_j's, and the errors in $T_{B,j}$'s as

$$\delta L_v = \delta a_0 + \sum_{j=1}^{2} (\delta a_j T_{B,j} + a_j \delta T_{B,j}) \tag{2}$$

where the subindex j = 1,2 refers to the WVR frequency channels. This article focuses primarily on errors in $T_{B,j}$ induced by tropospheric fluctuations. However, for the completeness of the discussion and because they are so large, sources of errors in a_j's are briefly summarized first.

The biggest errors in a_j's come from two sources: (1) inaccurate modeling of the absorptivity of water vapor, α_v [i.e., from errors of the dependence of $\alpha_v = \alpha_v(T, p, \rho, f)$ on the ambient temperature T, pressure p, water vapor density ρ, and frequency f], and (2) uncertainties in the spatial and temporal distributions of atmospheric pressure, temperature, and water vapor and liquid present in the troposphere during the observation along the line of sight. Errors in the a_j's cause scale errors in L_v, of the type $\delta L_v \simeq L_v \delta a_1 / a_1$. The error caused by inaccurate modeling of $\alpha_v(T, p, \rho, f)$ is systematic, about 10 percent for the current absorptivity models. Atmospheric profile uncertainties depend on season, site, weather, time of day, and line of sight. The uncertainties are difficult to model and are the reason why there is no one-to-one correspondence between the brightness temperature and the path delay. The error caused by uncertainties in atmospheric profiles is between 2 and 4 percent, depending upon the specific retrieval algorithm used. Several possibilities pertaining to the feasibility of reducing the δa_j's will be noted in Section V.

The error in the brightness temperature, $\delta T_{B,j}$, comes from two sources: (1) the error $\delta T_{A,j}$ in the measured WVR antenna temperature $T_{A,j}$, and (2) an error in the interpretation of $T_{A,j}$. The latter contribution to $\delta T_{B,j}$ originates in the fact that WVR's do not measure $T_{B,j}$ directly, but rather they record a signal, $V_{A,j}$ (from which $T_{A,j}$ is extracted), and the obtained $T_{A,j}$ is used to estimate the brightness temperature $T_{B,j}$. The error $\delta T_{A,j}$ in the WVR-measured $T_{A,j}$ can be expressed in terms of the WVR parameters, as follows: All WVR's use an internal reference, such as blackbody radiation or a noise diode, to enable a subtraction of the contribution of the system temperature from the recorded data. The recorded $V_{A,j}$ is proportional to the difference between $T_{A,j}$ and the reference load temperature, T_{ref},

$$V_{A,j} = g\,(T_{A,j} - T_{ref}) \tag{3}$$

where g is the WVR gain. Inverting Eq. (3) to obtain $T_{A,j}$ and taking a differential of the resulting equation yields the error $\delta T_{A,j}$ in the measured $T_{A,j}$

$$\delta T_{A,j} = \frac{\delta V_{A,j}}{g} + \delta T_{ref} - \frac{\delta g}{g^2} V_{A,j}$$

$$= \frac{\delta V_{A,j}}{g} + \delta T_{ref} + \frac{\delta g}{g}(T_{ref} - T_{A,j}) \tag{4}$$

Thus, $\delta T_{A,j}$ comes from three WVR parameters, the system noise (modeled as the uncertainty in the equivalent temperature, $\delta V_{A,j}/g$), and the uncertainties in the reference load temperature (δT_{ref}) and the WVR gain (δg). Figure 1 shows that for the path delay error to be less than 1 mm, the noise (or more generally, any unmonitored drifts) in all temperature-like quantities must be less than 0.2 K. In practice, the effect of the system noise on path delay estimates can be reduced (at the expense of time resolution) by increasing the signal integration time. As long as T_{ref} remains constant, the path delay error caused by using an incorrect value of T_{ref} is a constant bias (whose effect on astrometric estimates can be eliminated by differencing between the observations).

Because the antenna voltage $V_{A,j} \propto T_{A,j} - T_{ref}$, the error caused by δg [the last term on the right-hand side of Eq. (4)] consists of two terms. The first is $\propto T_{ref}$, the second is $\propto T_{A,j}$. Note that since the typical $T_{ref} \simeq 300$ K is bigger than $T_{A,j}$ ($T_{A,j} \simeq T_{B,j} \simeq 10$ to 100 K), the presence of T_{ref} in $V_{A,j}$ enhances the effect of the gain error (whatever its origin may be) on δL_v. By using Eq. (4) in Eq. (2), the first term (i.e., the term $\propto T_{ref}$) leads to $\delta L_v \propto a_i\, T_{ref}\, \delta g/g$. For stable gain (i.e., for a constant difference between the estimated and the WVR true gains), this is a constant bias. For unmonitored gain fluctuations, this is a random error, which, in order to satisfy the 1-mm path delay requirement (see Fig. 1), must be $\delta g/g < 0.08$ percent. The second term (i.e., the term $\propto T_{A,j}$) is a scale error, $\delta L_v \simeq L_v\, \delta g/g$, which is systematic for a stable gain and time varying for an unstable gain. This error depends on the tropospheric humidity and the observed elevation. For the error to be less than 1 mm, the gain error must be $\delta g/g < 0.1 \sin E / L_{v,z}$ (where $L_{v,z}$ is the zenith path delay in centimeters and $L_{v,z} = 6$ cm for a troposphere with 1 g/cm^2 of water vapor column density at zenith). Figure 1 shows that for the scale error to be less than 1 mm at a 10-deg elevation when $L_{v,z} = 6$ cm, $\delta g/g$ must be less than 0.26 percent. For the error to be less than 1 mm at $E = 6$ deg when $L_{v,z} = 24$ cm, $\delta g/g$ must be less than 0.04 percent.

The gain error can originate from several sources. The most troublesome of these are unmonitored instrumental drifts on a time scale of 100 to 1000 sec[4,5] (stochastic fluctuations on time scales much shorter than the radio observations can be incorporated into the system noise). However, since they originate in the instrument, the drifts should be controllable by improved instrument stabiliza-

[4] G. M. Resch (Tracking Systems and Applications Section) and S. Keihm (Microwave Observational Systems Section), personal communication, Jet Propulsion Laboratory, Pasadena, California, 1981.

[5] G. Parks, C. Ruf, and S. Keihm, "Advanced Water Vapor Radiometer: Definition Phase Study" (internal document), Jet Propulsion Laboratory, Pasadena, California, November 29, 1990.

tion in advanced WVR designs. Tropospheric fluctuations are another source of δg for WVR's calibrated using the tip curves. Even though this δg is stochastic in origin, the ensuing difference between the estimated and the actual WVR gains causes a systematic (bias and scale) error in L_v. The error depends on tropospheric humidity and calibration strategy and will be calculated in Section III of this article.

The other contribution to $\delta T_{B,j}$ is the error made in inferring $T_{B,j}$ from $T_{A,j}$. The simplest and most often used relationship between $T_{B,j}$ and $T_{A,j}$ is that $T_{B,j} = T_{A,j}$. This relationship can be in error because of inaccurate antenna pointing and spatial separation between the WVR antenna and the radio telescope. Another source of uncertainty is the effect of averaging tropospheric fluctuations over WVR beam intensity distribution. Section IV derives an expression for the error in the estimated $T_{B,j}$ that was caused by the beam averaging of tropospheric fluctuations for collocated and copointed antennas. The error will increase with decreasing elevation more rapidly than L_v, i.e., faster than a simple scale error. Since, as a result of this increase, low-elevation data will be weighted more heavily than they should be during VLBI data reduction, astrometric parameter estimates will be impacted.

III. Error in the WVR Gain Estimated From Tip Curves Due to Tropospheric Fluctuations

This section presents a calculation of the error in the estimated gain ($\hat{g}$) of WVR's induced by tropospheric fluctuations during the WVR calibration using the tip curves.[6,7] Tip curves use the elevation dependence of the sky brightness temperature [$T_{B,i} \equiv T_B(E_i)$, where E_i is the tip elevation] to calibrate the WVR gain. The WVR gain is determined by fitting the WVR recorded signal $V_{A,i}$ ($V_{A,i} \equiv V_A(E_i)$). If the elevation dependence of $T_{B,i}$, and therefore of $V_{A,i}$, were known, this calibration procedure would be limited only by thermal measurement noise. Spatial and temporal fluctuations of atmospheric water vapor cause the actual distribution of water vapor to depart from the static distribution assumed in fitting the $V_{A,i}$'s. Therefore, an error due to tropospheric fluctuations is introduced into the gains estimated from the tip curve data. All delays calculated with the derived gain will, therefore, also be in error. In this section, the covariance of the gain estimates is determined in terms of the covariance of the tropospheric opacity. This is done by performing a tip-curve analysis of modeled data and evaluating the opacity covariance by using the Kolmogorov turbulence model [1] for the wet troposphere.

A. Tip-Curve Analysis

The tip-curve data were modeled by using the optically thin tropospheric approximation for the standard radiation transport equation, neglecting the effect of the Earth's curvature, ray bending, and nonzero WVR beamwidth, assuming negligible time elapsed during each tip curve sequence, and neglecting the time variation of all other model parameters except the tropospheric opacity. The recorded signal $V_{A,i}(t)$ for tip curve epoch t at elevation E_i is then expressed as [5]

$$\begin{aligned} V_{A,i}(t) &= g\ (T_{B,i}(t) - T_{ref}) \\ &= g\ \left(T_C\ e^{-\tau_i(t)} + T_M(1 - e^{-\tau_i(t)}) - T_{ref}\right) \\ &\simeq g\ (T_C\ +\ T_{MC}\ \tau_i(t)\ -T_{ref}) \end{aligned} \tag{5}$$

where the subscript i refers to ith elevation, g is the WVR gain, T_{ref} ($T_{ref} \simeq 300$ K) is the reference temperature discussed in Section II, $T_C \simeq 2.8$ K is the cosmic background temperature, $T_{MC} = T_M - T_C$ where $T_M \simeq 270$ to 280 K is the average atmospheric temperature [5], and $\tau_i(t)$ ($\tau_i(t) = \tau(E_i, t)$) is a time-varying line of sight opacity at elevation E_i. The linear approximation [the second expression on the right-hand side of Eq. (5)] is a good approximation for most optically thin ($\tau_i < 0.5$) tropospheres of interest, with the added benefit of mathematical simplicity.

In the standard tip curve analysis, the method of least squares [6] is used to obtain the gain estimate ($\hat{g}$) in terms of the tip data. Appendix A discusses the tip curve fitting in detail. The data are fit to a static (temporally averaged) version of Eq. (5) by using the mapping function $\langle\tau_i\rangle = \tau_z\ A_i$, where $\langle ... \rangle$ designates the statistical average, τ_z is the averaged opacity mapped to zenith, and the air mass $A_i = 1/\sin E_i$. For N elevations, the fitting leads to an equation of the following type:

$$\hat{g}(t)\ =\ \sum_{i=1}^{N} c_i\ V_{A,i}(t) \tag{6}$$

[6] J. Z. Wilcox, "The Standard Deviation of WVR Gain Estimated from Tip Curves due to Wet Troposphere Fluctuations," JPL Interoffice Memorandum 335.6-91-032 (internal document), Jet Propulsion Laboratory, Pasadena, California, December 19, 1991.

[7] J. Z. Wilcox, "The Difference Between Two Successive WVR Gain Estimates From Tip Curves due to Wet Troposphere Fluctuations," JPL Interoffice Memorandum 335.6-91-033 (internal document), Jet Propulsion Laboratory, Pasadena, California, December 20, 1991.

where c_i's are coefficients that depend on the assumed T_C, T_{MC}, and T_{ref}, and on the so-called variance–covariance matrix $W^{-1} \equiv \mathrm{cov}(V_A(t), V_A(t'))$ (See [6] and Appendix A). Taking Eq. (6) at t and t' and substituting Eq. (5), the covariance of the gain estimates separated by the time interval $T = t - t'$ is obtained in terms of opacity correlations as

$$\mathrm{cov}(\hat{g}(t), \hat{g}(t')) = \sum_{i,j=1}^{N} c_i\, c_j\, \mathrm{cov}(V_{A,i}(t) V_{A,i}(t'))$$

$$\simeq g^2\, T_{MC}^2 \sum_{i,j=1}^{N} c_i\, c_j\, \mathrm{cov}(\tau_i(t)\tau_j(t')) \quad (7)$$

The opacity covariance $\mathrm{cov}(\tau_i(t)\tau_j(t'))$ was evaluated by neglecting fluctuations in the dry component of $\tau_i(t)$ (dry troposphere contributes less than about 30 percent of the total opacity fluctuations)[8] and by describing the fluctuations in the wet component by Kolmogorov turbulence [1]. Specifically, the wet contribution to τ_i was expressed as the line-of-sight integral $\tau_{v,i} = \int_0^{A_i h_v} \alpha_v(\vec{r}_i, t)\, dr_i$, where $\alpha_v(\vec{r}, t)$ is the tropospheric absorptivity due to water vapor per unit length at $\vec{r}$, $dr_i = A_i dz$ is the path increment along the line of sight at elevation E_i, and h_v is the wet troposphere height. Using $\alpha_v(\vec{r}, t) \simeq \chi(\vec{r}, t)\tau_{v,z}/L_{v,z}$, where χ = index of refraction − 1, and $\tau_{v,z}$ and $L_{v,z}$ are wet opacity and path delay at zenith, respectively, Appendix B shows explicitly the integral expressions that relate $\mathrm{cov}(\tau_i(t)\tau_j(t'))$ to the structure functions for $\chi(\vec{r}, t)$. (Note that $L_{v,z} \simeq 6$ cm, and $\tau_{v,z} \simeq 0.04$ and 0.02 per 1 g/cm^2 of zenith water vapor column density, and the dry opacity $\tau_{d,z} \simeq 0.017$ and 0.04, at 20.6 GHz and 31.4 GHz, respectively.) The refractivity structure functions were evaluated by generalizing the Kolmogorov turbulence expression [1] for the structure function $\left\langle (\chi(\vec{r}) - \chi(\vec{r} + \vec{R}))^2 \right\rangle$ to inhomogeneities correlated both spatially and temporally [1]:[9]

$$D_\chi(\vec{R}, T) \equiv \left\langle \left(\chi(\vec{r}, t) - \chi(\vec{r} + \vec{R}, t + T) \right)^2 \right\rangle$$

$$= \frac{N_v^2\, C^2\, |\vec{R} + \vec{v}\, T|^{2/3}}{1 + (|\vec{R} + \vec{v}\, T|/L_s)^{2/3}} \quad (8)$$

where $\vec{R}$ and T are the spatial and temporal intervals over which the structure function is evaluated and $\vec{v}$ is the wind velocity. The role of Eq. (8) in VLBI data reduction was discussed in [1]. By using the standard deviation for retrieved path delays at average DSN conditions, the turbulence strength was shown to be $C = 2.4 \times 10^{-7}\mathrm{m}^{-1/3}$ for a tropospheric slab with a water vapor column density of $N_v \simeq 1$ g/cm^2 at zenith (corresponding to approximately 6 cm of wet path delay) and height $h_v = 1$ km [1]. For $h_v = 2$ km, the recalculated $C = 1.1 \times 10^{-7}\mathrm{m}^{-1/3}$, which is the value used in this article.[10] The turbulence saturation scale length was taken to be $L_s = 3{,}000$ km [1]. The temporal correlation depends on the wind velocity v (Reference [1] shows that if one identifies T with $|\vec{R}|/v$, the spatial correlation between two parallel lines of sight separated by the distance $|\vec{R}|$ projected on the Earth's surface is equal to the temporal correlation of a single line of sight at time t and later $t+T$.) This article used $v = 10$ m/sec, which is a typical wind speed at the Goldstone DSN antenna site.

B. The Estimated Gain Error

The standard deviation of the estimated gain, $\sigma_{\hat{g}}$, is equal to the square root of the covariance given by Eq. (7) for $t = t'$. For $t \neq t'$, Eq. (7) gives the gain covariance as a function of the time interval $T = |t - t'|$ between two successive gain estimates, $\sigma_{\hat{g}}(T) \equiv (\mathrm{cov}(\hat{g}(t), \hat{g}(t+T)))^{1/2}$. Before discussing the numerical results, note that Eq. (7) depends on the number (N) of tip elevations. Evaluating Eq. (7) for $N = 2$, 3, and 4, the covariance was found to depend on the tip range and be nearly independent of the elevation distribution within the range.[11] That is, the covariance is determined by the least-correlated tropospheric inhomogeneities (i.e., by correlations between the lines of sight associated with the minimum, E_{min}, and maximum, E_{max}, tip elevations). In what follows, the errors will be shown versus E_{min} (with E_{max} at zenith) per 1 g/cm^2 of zenith column density of water vapor present in the troposphere during WVR calibration. Note that because they are proportional to N_v, the errors are minimized by calibration in dry (and stable) weather.

The value of $\sigma_{\hat{g}}$ is shown in Fig. 2 as a function of E_{min}. The error has a flat minimum of approximately 0.26 percent between approximately $E_{min} = 10$ deg and 30 deg. Below a 10-deg elevation, the error increases with decreasing E_{min} because the decorrelation between the tropospheric fluctuations associated with E_{min} and 90-deg lines of sight increases more rapidly than does the air mass difference. Above a 30-deg elevation, the opposite is true. It can be shown that as E_{min} approaches 90 deg, the error increases as $(90 - E_{min})^{-3/2}$ (which is slower than it

[8] G. E. Lanyi, personal communication, Tracking Systems and Applications Section, Jet Propulsion Laboratory, Pasadena, California, 1991.

[9] See Footnote 7.

[10] See Footnote 6.

[11] See Footnote 6.

would be if the fluctuations were completely random, in which case the error would increase as $(90 - E_{min})^{-2}$). Thus, to minimize the gain error, E_{min} should be between 10 and 30 deg.

The least-squares fit coefficients c_i's depend on the variance–covariance matrix W^{-1}. In the so-called consider analysis, the observable errors are assumed to be uncorrelated, and W^{-1} is approximated by a unit diagonal [1]. Using the observable variance–covariance matrix W^{-1} minimizes the variance of the estimated gain, Eq. (7) (i.e., it minimizes $\sigma_{\hat{g}}$). The errors calculated by using the unit and observable variance–covariance matrix W^{-1} are shown as solid and broken line curves, respectively, in Fig. 2. Note that the two curves are practically the same in the minimum region and differ by 8 percent at most in the wings. This indicates that using the full covariance–variance matrix W^{-1} does not significantly improve the estimated gain accuracy.

Figure 3 shows the temporal development of $\sigma_{\hat{g}}(T)$. The value of $\sigma_{\hat{g}}(T)$ decreases at $T << T_{corr}$ approximately as $\sigma_{\hat{g}}(T) \simeq \sigma_{\hat{g}}\sqrt{1-(2T/T_{corr})}$, where T_{corr} is the decorrelation time. (Note that in Fig. 3, $\sigma_{\hat{g}}(T_{corr}/2) \simeq \sigma_{\hat{g}}/2$.) The value of T_{corr} depends on v and E_{min} as $T_{corr} \simeq h_v/(v \tan E_{min})$. That is, T_{corr} is the time it takes for a "frozen" troposphere [1] to pass through the tip range between E_{min} and zenith. For $v = 10$ m/sec, and $E_{min} \simeq 30$ deg, T_{corr} is about 7 min. The single-gain estimate errors ($\sigma_{\hat{g}}$'s) become independent from each other when the time T between subsequent tip curves exceeds T_{corr}. Therefore, if one wishes to minimize the estimated gain error by tip curve repetition, the tip curves should be separated by a time interval greater than 7 min.

C. The Estimated Path Delay Error

It has already been discussed in Section II that a WVR gain error induces two types of errors in the estimated L_v: a bias and a scale error. Using Eq. (4) in Eq. (2) and designating the bias and scale errors as ΔL_v and δL_v, respectively, the two errors are

$$\Delta L_v(\text{cm}) \simeq (a_1 + a_2)\, T_{ref}\, \frac{\sigma_{\hat{g}}}{g}$$

$$\simeq 120\frac{\sigma_{\hat{g}}}{g} \simeq 0.3\, N_{v,cal} \qquad (9a)$$

$$\delta L_v(cm) \simeq (a_1\, T_{A,1} + a_2\, T_{A,2})\frac{\sigma_{\hat{g}}}{g}$$

$$\simeq L_v \frac{\sigma_{\hat{g}}}{g} \simeq 0.016\, \frac{N_{v,cal} N_{v,obs}}{\sin E} \qquad (9b)$$

where the gain estimates at 20.6 GHz and 31.4 GHz were assumed to be correlated (i.e., the gains in the two WVR channels were determined during the same tip sequence) and their magnitudes the same. $T_{ref} = 300$ K, $N_{v,cal}$ and $N_{v,obs}$ are the number of grams per cm^2 of the column density of water vapor at zenith during the WVR calibration and radio observation, respectively, E is the elevation of the observation, and the last expressions on the right-hand sides correspond to the minimum $\sigma_{\hat{g}}/g \simeq 0.26$ percent. The ΔL_v corresponding to $N_{v,cal} = 1$ g/cm^2 (i.e., to $L_{v,z} = 6$ cm) is shown in Fig. 2. The minimum ΔL_v is approximately 3 mm. Note that as long as the WVR gain remains constant, ΔL_v is also constant, which makes it possible to remove its effect on astrometric estimates and delay rates by differencing between observations. For unstable gain, the gain changes must be monitored (to achieve a 1-mm path delay accuracy) with 0.08 percent accuracy. The dependence of the scale error (strictly speaking, δL_v will be a pure scale error only in optically thin tropospheres) on elevation was shown in Fig. 1. The value of δL_v caused by a 0.26-percent gain error at a 10-deg elevation when $N_{v,obs} = 1$ g/cm^2 is approximately 1 mm; when $N_{v,obs} = 4$ g/cm^2, the error is 4 mm. To reduce δL_v to 1 mm, the gain error will have to be reduced by using a different calibration technique, tip curve repetition, or a parameter estimation during the data analysis. How this can be accomplished for a stable WVR is discussed in Section V of this article.

A note should be made here on the dependence of ΔL_v and δL_v on T_{ref}. From Eq. (9a), it would seem that $\Delta L_v \propto T_{ref}$. However, by performing the least-squares analysis, one finds that the tropospheric fluctuation-induced $\sigma_{\hat{g}}$ is $\propto 1/T_{ref}$. This cancels the dependence of ΔL_v on T_{ref} and makes $\delta L_v \propto 1/T_{ref}$. [Note, however, that ΔL_v caused by an *instrumental* gain drift will be $\propto T_{ref}$, as given by the first expression on the right-hand side of Eq. (9a).]

IV. Error in the Estimated Brightness Due to the WVR Nonzero Beamwidth

Retrieval algorithms relate the line of sight L_v to the brightness temperature (T_B) in the same direction, whereas data recorded by the WVR's are beam averaged around the WVR pointing direction. For collocated and copointed WVR antennas and radio telescopes (the telescope points along the line of sight to the radio source), the copointing introduces two types of errors into the estimated T_B: a systematic error due to the nonlinear dependence of air mass on elevation and a random error due to WVR beam

averaging of tropospheric fluctuations.[12] The systematic error can be calculated for known beam intensity distributions (beam shapes) and water vapor content in the troposphere. Its effect on path delay estimates can be eliminated by pointing the WVR to a slightly higher elevation so that the radio source lies in the direction of the centroid of the distribution of WVR beam brightness. In this section, the direction of the brightness centroid is calculated by WVR beam averaging of the air mass [see Eq. (12) for the centroid definition], and the random error is determined by using the tropospheric opacity statistically as in Section III. It has been suggested that to simplify WVR beam steering for collocated antennas, radio telescope and WVR antennas should be copointed.[13] After correcting the WVR data by subtracting from them the systematic error, the "corrected" data would be used to estimate path delays in the direction of the beam's geometrical center. Therefore, the random error has been evaluated also for this geometrical center pointing case (and found that it is bigger than the random error for the brightness centroid pointing, by an amount that depends on the WVR beamwidth and elevation).

Before presenting numerical results, the WVR beam intensity distribution must be specified. The systematic error for an assumed Gaussian beam with 7.5-deg full width at half maximum (FWHM) has been calculated previously.[14] To simplify the computations, and since the aim of this article is to provide error estimates (rather than to tailor the errors to specific WVR beam designs), a beam is used whose cross section when viewed in the propagation direction is a square with sharp cutoffs for the beam intensity. Specifically, for a beam centered at elevation E_c and azimuth φ_c, the WVR antenna temperature, $T_A(E_c)$, is calculated by integrating the brightness temperature of the sky ($T_B(E)$) over the intensity distribution:

$$T_A(E_c) \equiv [T_B]_c \simeq \int\int B_c(E,\varphi)\, T_B(E)\, dE\, \cos E\, d\varphi \tag{10}$$

where $[\ldots]_c$ signifies the WVR beam average around (E_c, φ_c), E and φ are elevation and azimuth angles, respectively, and $B_c(E,\varphi)$ is the WVR antenna beam radiation pattern

$$B_c(E,\varphi) \simeq \frac{1}{(2\,\Delta_{1/2})^2} \quad \ldots$$

$$\text{when } |E - E_c| \le \Delta_{1/2} \text{ and } |\varphi - \varphi_c| \le \frac{\Delta_{1/2}}{\cos E} \tag{11}$$

and zero otherwise, and $\Delta_{1/2}$ = FWHM/2 is the WVR beam half-width. Note that as long as $E_c > \Delta_{1/2}$, ground pickup is avoided for this WVR beam pattern. By comparing the numerical results, the systematic error calculated using beam intensity distribution with sharp cutoffs (for the same FWHM) is about 20–30 percent smaller than for the Gaussian beams. (It was also found that neglecting beam spreading in the azimuthal direction underestimates the random error by less than 10 percent.) The radio telescope beam was approximated by an infinitely narrow pencil beam. Since the errors are proportional to tropospheric water vapor, all shown errors are for 1 g/cm^2 of zenith water vapor column density.

A. Tropospheric Fluctuation–Induced Error for Brightness Centroid Pointing

The elevation E_b of the WVR beam brightness centroid is determined by requiring that the statistically averaged brightness temperature $\langle T_B(E_b)\rangle$ at the centroid elevation E_b be equal to the WVR antenna temperature $\langle T_A(E_c)\rangle$

$$\langle T_B(E_b)\rangle = \langle T_A(E_c)\rangle \tag{12}$$

where E_c is the elevation of the WVR beam geometrical center, and $\langle\ldots\rangle$ designates the statistical average. Substituting $T_B(E)$ [Eq. (5)] into Eq. (10), neglecting the effect of ray bending and the Earth's curvature, and using the optically thin troposphere approximation, the statistically averaged antenna temperature is

$$\langle T_A(E_c)\rangle = T_C + T_{MC}\, \tau_z\, [A]_c \tag{13}$$

where the WVR beam averaged air mass $[A]_c$ is given by the same integral expression as Eq. (10) except that $T_B(E)$ is replaced by $A_E = 1/\sin E$. By also using Eq. (5) for $T_B(E_b)$ in Eq. (12), one obtains the result that in an optically thin troposphere, the brightness centroid coincides with the air mass centroid,

$$\frac{1}{\sin E_b} = \int \frac{B_c(E,\varphi)}{\sin E}\, dE\, \cos E\, d\varphi \tag{14}$$

[12] J. Z. Wilcox, "The Error in the Estimated Path Delay due to WVR Antenna Beam Width: Beam Averaged Air Mass and Wet Troposphere Fluctuations Effects," JPL Interoffice Memorandum 335.6-92-004 (internal document), Jet Propulsion Laboratory, Pasadena, California, January 31, 1992.

[13] See Footnotes 4 and 5.

[14] S. Robinson, "A Simple Analytic Correction for WVR Beam Width," JPL Interoffice Memorandum 335.4-530 (internal document), Jet Propulsion Laboratory, Pasadena, California, July 23, 1985.

The calculated difference (the offset) between E_c and E_b is shown in Fig. 4. The offset is always positive (i.e., the brightness centroid is tilted from the beam's geometrical center to a lower elevation), it increases with the beam width approximately as $\Delta_{1/2}^2$, and it has a very wide minimum in the elevation range around $E_c \simeq 52$ deg. The minimum occurs because the systematic error, and hence the offset, depends on a nonvanishing second derivative of A_E versus E. Specifically, for $E < 90 - \Delta_{1/2}$, the offset $E_c - E_b \simeq (\Delta_{1/2}^2/6)A_c''/A_c'$, where A_c' and A_c'' are the first and second derivatives of $A_E = 1/\sin E$ versus E at E_c. Since A_c''/A_c' has a local minimum at 52 deg, the offset has also a local minimum at 52 deg. Note also that as E_c approaches 90 deg, the offset rapidly increases to $\Delta_{1/2}/\sqrt{3}$. For the current WVR $\Delta_{1/2} < 4$ deg, the offset is less than 0.2 deg in the elevation range between approximately 20 and 80 deg. Note that in an optically thick troposphere, the brightness centroid will differ somewhat from the air mass centroid. This is a consequence of the nonlinear dependence of T_B on the air mass, Eq. (5), in an optically thick atmosphere.

The error in the estimated $T_B(E_b)$ is the square root of the variance

$$\sigma_T^2(E_b) = \langle (T_A(E_c) - T_B(E_b))^2 \rangle = \left\langle \left(\int T_B(E)\ (B_c(E,\varphi) - \delta(E - E_b, \varphi - \varphi_b))\ dE\ \cos E\ d\varphi \right)^2 \right\rangle \qquad (15)$$

where $\delta(E-E_b, \varphi-\varphi_b)$ is the Dirac delta function centered at (E_b, φ_b). Equation (15) was evaluated by expressing $T_B(E)$ using Eq. (5), and then evaluating the correlations between the tropospheric opacities using the Kolmogorov turbulence model, as described in the paragraph following Eq. (7). The corresponding path delay error $(\sigma_{L,v}(E_b))$ was obtained by substituting $\sigma_T(E_b)$ into Eq. (2), where $\sigma_T(E_b)$'s were identified with $\delta T_{B,j}$'s ($j = 1, 2$ designates 20.6- and 31.4-GHz frequency channels, respectively) for the two WVR frequencies. Figure 5(a) plots the path delay error versus E_c. Note that the error increases with decreasing elevations faster than L_v. The error is plotted versus $\Delta_{1/2}$ in Fig. 5(b). After a rapid rise near zero, the error increases sublinearly. At $\Delta_{1/2} \simeq 3$ deg and $E_c = 30$ deg, 20 deg, and 10 deg, the errors are 0.06 cm, 0.1 cm, and 0.3 cm, respectively. Advanced WVR's with narrow beamwidths were designed for observations at low elevations. For $\Delta_{1/2} = 1$ deg, the errors are approximately 0.23 cm and 0.5 cm at $E_c = 10$ deg and 6 deg, respectively. These results qualitatively agree with errors calculated for copointed beams.[15]

The error shown in Fig. 4 refers to instantaneous measurements. However, astrometric data are averaged over time intervals on the order of 1 to 2 minutes, which tends to average out the fluctuations. Assuming that the radio telescope and the WVR observe simultaneously and continuously during t_{int}, the time averaged $T_B(E)$ is

$$\bar{T}_B(E) = \frac{1}{t_{int}} \int_0^{t_{int}} dt\ T_B(E,t) \qquad (16)$$

Using $\bar{T}_B(E)$ instead of $T_B(E)$ on the right-hand side of Eq. (15), the result is shown in Fig. 6. At $t_{int} < T_{1/2}$, the error decreases with a time constant $T_{1/2} \simeq 2\ \Delta_{1/2} h_v/v\ \sin^2 E_c$, which is the time required for the moving troposphere to pass through the WVR beam cone (and thus erase the tropospheric differences between the beam averaged and line-of-sight opacities). The value of the time constant $T_{1/2}$ increases with decreasing elevation and increasing half-width. For $h_v = 2$ km, $v = 10$ m/sec, $\Delta_{1/2} = 3$ deg, and $E_c = 30$ deg and 10 deg, $T_{1/2}$ is approximately 1.5 min and 12 min, respectively. For $\Delta_{1/2} \simeq 0.1$ deg, $T_{1/2}$ is 3 sec and 25 sec, respectively. Obviously, so that the time resolution is not degraded, WVR integration should never be longer than radio telescope integration.

B. Tropospheric Fluctuation–Induced Error for Geometrical Center Pointing

The systematic and random errors for a copointed radio telescope and a WVR antenna are calculated next. The usual argument for why WVR data should be associated with the direction of the beam's the brightness centroid is that for a constant troposphere, $\langle T_A(E_c) \rangle = \langle T_B(E_b) \rangle$. If this were the only criterion, one could also correct the WVR data (i.e., $T_A(E_c)$) by subtracting from them the estimated value of the difference between $\langle T_A(E_c) \rangle$ and $\langle T_B(E_c) \rangle$ and identify this "corrected" data as the actual value of the brightness temperature $T_B(E_c)$ in the direc-

[15] S. Keihm, "Finite Beam Effects on LOS Path Delay Decorrelation," (internal document), Jet Propulsion Laboratory, Pasadena, California, March 22, 1990.

tion of the beam's geometrical center. For a copointed radio telescope and a WVR antenna, the (systematic) difference $\Delta T_A(E_c)$, is determined as

$$\Delta T_A(E_c) \equiv \langle T_A(E_c) - T_B(E_c) \rangle = T_{MC}\ \tau_z\ \Delta A_c \qquad (17)$$

where τ_z is the total (wet and dry) zenith opacity, and $\Delta A_c \equiv [A]_c - A(E_c)$ is the difference between the beam averaged and geometrical center air mass. Note that $\langle T_A(E_c) \rangle$ is bigger than $\langle T_B(E_c) \rangle$.

The value of $\Delta T_A(E_c)$ at 20.6 GHz (and the corresponding path delay error) is shown in Fig. 7. The error increases with beamwidth approximately as $\Delta_{1/2}^2$. Note that for the radiation pattern with a sharp cutoff for intensity distribution, this quadratic dependence on $\Delta_{1/2}$ can be derived analytically

$$\Delta A_c = \frac{1}{2\ \Delta_{1/2}} \ln \frac{\tan(E_c + \Delta_{1/2})/2}{\tan(E_c - \Delta_{1/2})/2} - A_c$$

$$\simeq \frac{\Delta_{1/2}^2}{6\ \sin E_c} \left(1 + \frac{2}{\tan^2 E_c}\right) \qquad (18)$$

where the approximate equality on the right-hand side has been obtained for narrow line widths, $\Delta_{1/2} << E_c$. The more important feature to notice in Fig. 7 is that the error increases with decreasing E_c more rapidly than L_v, namely that $\Delta L_v \propto \Delta T_A(E_c) \propto \Delta A_c \propto (1 + 2/\tan^2 E_c)/\sin E_c$. This is the same type of increase as for the random error calculated in the preceeding paragraphs, i.e., the errors caused by WVR beam averaging increase with decreasing elevation more rapidly than a simple scale error. At $\Delta_{1/2} \simeq 3$ deg and $E_c = 30$ deg, 20 deg, and 10 deg, the systematic path delay error is approximately 0.36 mm, 1.2 mm, and 10 mm, respectively. The error decreases with decreasing beam width. At $\Delta_{1/2} \simeq 1$ deg and $E_c = 10$ deg and 6 deg, the error is 2 mm and 6 mm, respectively. (At $\Delta_{1/2} \simeq 0.1$ deg, the error is 0.1 mm and 0.06 mm, respectively.)

Correcting the measured $T_A(E_c)$ by $\Delta T_A(E_c)$, the stochastic error in the inferred $T_B(E_c)$ is determined from

$$\sigma_T^2(E_c) = \langle (T_A(E_c) - \Delta T_A(E_c) - T_B(E_c))^2 \rangle$$
$$= \left\langle \left(\int (T_B(E) - \langle T_B(E) \rangle)\ (B_c(E,\varphi) - \delta(E - E_c, \varphi - \varphi_c))\ dE\ \cos\ E\ d\varphi \right)^2 \right\rangle \qquad (19)$$

where $\delta(E - E_c, \varphi - \varphi_c)$ is the Dirac delta function centered at (E_c, φ_c). Equation (19) was evaluated by using the same procedure as Eq. (15). The corresponding path delay error ($\sigma_{L,v}(E_c)$) is shown in Fig. 8(a) versus E_c and in Figure 8(b) versus $\Delta_{1/2}$. Similarly as for the systematic error [and for the stochastic error for the brightness centroid, $\sigma_{L,v}(E_b)$], $\sigma_{L,v}(E_c)$ increases with decreasing E_c more rapidly than L_v. Note that when the systematic error is smaller than $\sigma_{L,v}(E_b)$ (such as for $\Delta_{1/2} < 1$ deg at a 6-deg elevation, or for $\Delta_{1/2} < 1.5$ deg at a 10-deg elevation), $\sigma_{L,v}(E_c)$ is about the same as $\sigma_{L,v}(E_b)$; whereas when the systematic error is bigger than $\sigma_{L,v}(E_b)$, $\sigma_{L,v}(E_c)$ looks more like the systematic error (which increases $\propto \Delta_{1/2}^2$ and can become very large). That is, while the copointing will significantly increase the stochastic error for wide WVR beams, the increase will be small for narrow beams. It has also been found that when $\sigma_{L,v}(E_c) \simeq \sigma_{L,v}(E_b)$ (the narrow beam case), the $\sigma_{L,v}(E_c)$ for the integrated signal [as in Eq. (16)] decreases with t_{int} at about the same rate as does $\sigma_{L,v}(E_b)$; whereas when $\sigma_{L,v}(E_c) > \sigma_{L,v}(E_b)$ (the wide beam case), the decrease is significantly slower.[16] Thus, when the systematic error is less than $\sigma_{L,v}(E_b)$ (the narrow beam case, $\Delta_{1/2} < 1$ deg for all $E > 6$ deg), the copointing will introduce a negligible error into the estimated path delays using WVR's. However, for beam sizes greater than 1 deg, the WVR's should be pointed at a slightly higher elevation than the radio telescope.

V. Discussion and Recommendations

The main goal of this article is to investigate how tropospheric dynamics affect the ability of realistic WVR's to track tropospheric fluctuations. Two effects were studied in detail: errors in WVR instrument gain calibration from tip curves and errors in the estimated brightness temperature caused by WVR beamwidth averaging. The errors can be used to derive WVR gain stability requirements

[16] See Footnote 12.

and WVR antenna beamwidth that would make it possible to reduce the path delay error to the 1-mm level in the elevation range from zenith to 6 deg.

The minimum error induced by tropospheric fluctuations in a single gain estimate (per 1 g/cm^2 of zenith water vapor column density during WVR calibration) is approximately 0.26 percent. That error causes two types of errors in the estimated path delay. The first error, approximately 3 mm, is independent of path delay. Provided that the WVR gain remains constant, this is a bias error that can be removed by differencing between VLBI observations (biases have no effect on delay rates used for gravitational wave searches). The second error, $\delta L_v \simeq L_v \, \sigma_{\dot{g}}/g$, is a scale error. Figure 9 shows the scale error for a single gain estimate δL_v (mm) $\simeq 0.16 \; N_{v,cal} N_{v,obs} / \sin E$ (where $N_{v,cal}$ and $N_{v,obs}$ come from water vapor content during the WVR calibration and radiometric observation) as a function of $N_{v,cal} N_{v,obs}$ and elevation (E) of the radiometric observation. For example, assuming that $N_{v,cal} = 1$ g/cm^2 (corresponding to $L_{v,z} = 6$ cm) and $N_{v,obs} = 2$ g/cm^2, δL_v exceeds 3 mm (i.e., it exceeds the L_v-independent error) when $E \leq 6$ deg. When $N_{v,cal} = N_{v,obs} = 2$ g/cm^2, δL_v exceeds 6.2 mm at $E = 6$ deg. To achieve the desired 1-mm path delay accuracy, either the effect of δL_v on astrometric estimates or δg itself must be reduced. The success of any approach to obtaining accurate astrometric estimates depends on the stability of the WVR gain.

For a stable WVR gain, the scale error is systematic. Preliminary results of attempts to reduce the effect of systematic scale errors on astrometric estimates with VLBI data analysis appear to be promising, although more work is needed to ascertain quantitative results.[17] The gain error can be reduced by using an alternate gain calibration technique (such as two absolute reference load calibrations), or, assuming that the error induced by tropospheric fluctuations is the dominant error source, by tip curve repetition. Uncertainties in alternate calibration methods have so far prevented circumvention of tip curves. To reduce the error by tip curve repetition, the WVR gain must be sufficiently stable. For example, to achieve a 1-mm path delay accuracy at a 6-deg elevation when $N_{v,obs} = 2$ g/cm^2, the gain error must be less than 0.08 percent. To reduce the gain error to 0.08 percent when $N_{v,cal} = 2$ g/cm^2, the tip curve must be repeated at least $(0.52/0.08)^2 = 40$ times. Section III showed that successive gain estimates become decorrelated within a typical T_{corr} of approximately 7 min. Therefore, if one attempts to reduce the gain error by tip curve repetition, the tip curves should be separated by a time interval greater than 7 min, and the WVR gain should change by no more than 0.08 percent over at least 40 $T_{corr} \simeq 5$ hr.[18] (Because of the effect of other error sources and the possibility of humidity higher than 2 g/cm^2, the recommended WVR stability is 0.04 percent over the 5-hour period.) In the time interval between the WVR calibration and the radio metric observations (and during the observations) the gain will still have to be updated, e.g., by comparing the number of counts for the reference load.[19,20]

The error in the estimated brightness temperature due to WVR beam averaging of tropospheric fluctuations was found to be smaller when the direction of the radio source coincided with the WVR beam brightness centroid than with the beam geometrical center. The error increases with tropospheric water vapor content and beamwidth. More important, however, is that the error increases with decreasing elevation faster than L_v. Since low-elevation data will be weighted more heavily than they should be, this will affect astrometric estimates. Advanced WVR designs have been suggested to reduce the error and avoid ground pickup by implementing narrow beams. Figure 10 shows the errors in the two-dimensional space of beam half-widths ($\Delta_{1/2}$) and elevations for 1 g/cm^2 of zenith water vapor column density. For each curve, the error is less than the cutoff error for all $\Delta_{1/2}$'s and E's below and to the right of the curve. For example, for the error to be less than 1 mm at all $E > 10$ deg, $\Delta_{1/2}$ should be < 0.1 deg. For more humid weather, the errors will be higher (and the beamwidth requirement more stringent), proportional to zenith water vapor. Because of various approximations involved in deriving Fig. 10 (the WVR beam radiation pattern with sharp cutoffs for intensity distribution, an infinitely narrow pencil beam for the radio telescope, and an optically thin troposphere), the guidelines are approximate (the guidelines can easily be quantified by applying the methods described in this article to specific beam shapes).

Signal integration reduces the fluctuation-induced error from its instantaneous value with a time constant $T_{1/2} \simeq 2 \; \Delta_{1/2} \; h_v / v \sin^2 E$. Because of its dependence on beam width and elevation, the effect of signal integra-

[17] R. Linfield, Tracking Systems and Applications Section, personal communication, Jet Propulsion Laboratory, Pasadena, California, 1991.

[18] The measured gain of the current J and D series WVR's drift at a rate that causes an approximate 0.3-percent gain change in 1000 sec (Footnotes 4 and 5). Therefore, the stability of these WVR's should be improved by a factor of at least 60, from $\dot{g}/g \simeq 3 \times 10^{-6}$ sec^{-1} to $\dot{g}/g \simeq 5 \times 10^{-8}$ sec^{-1}.

[19] See Footnote 2.

[20] See Footnote 4.

tion has been neglected in Fig. 10. For example, for a WVR beamwidth $\Delta_{1/2} = 0.1$ deg (FWHM = 0.2 deg) and $E = 6$ deg, $T_{1/2}$ is 1 min, and the path delay error when $N_{v,obs} = 2$ g/cm^2 is about 4 mm. Hence, integrating the WVR signal over a 2-min period (which is a typical VLBI integration time) will reduce the fluctuation error to about 1 mm (which is the desired accuracy for the estimated path delays). It has been suggested that copointing a radio telescope and a WVR antenna in the same direction would simplify WVR antenna steering. The copointing will introduce a systematic error and increase the random error in the estimated path delay. For $E > 6$ deg, these additional errors will be smaller than the random error for the brightness centroid pointing for all beam sizes $\Delta_{1/2} < 1$ deg. For $\Delta_{1/2} > 1$ deg, the additional errors will increase $\propto \Delta_{1/2}^2$, and, in addition, the required WVR signal integration time to average out the fluctuation-induced error becomes longer[21] than the $T_{1/2}$ for the brightness centroid pointing (and longer than the VLBI integration time of about 2 min). Therefore, the ability for the wide beam WVR's to be pointed at a slightly higher elevation than the radio telescope is important.

[21] See Footnote 12.

From the brief discussion of various error sources in Section II, the biggest error in the estimated path delay is at the present time due to inaccurate modeling of the absorptivity of water vapor and uncertainties in the distribution of atmospheric parameters along the observed lines of sight (atmospheric noise). These uncertainties cause scale errors (see Fig. 1) in the estimated path delay: a systematic error of about 10 percent due to the error in the absorptivity model and between 2 and 4 percent random error due to atmospheric noise. To satisfy the 1-mm path delay accuracy requirement at a 6-deg elevation, the atmospheric noise must be reduced to the 0.17-percent level by, for example, custom tailoring the retrieval algorithm coefficients to specific sites and a set of observing conditions.

The accuracy of the present absorptivity models could be improved by better modeling and model calibration, using for example, a comparison of WVR and radiosonde data, direct measurements or estimates using interferometric data reduction of atmospheric path delays, or measurement of water vapor absorptivity in a laboratory-controlled environment. Investigation of some of these possibilities, including that of developing mathematical methods to filter out the effect of the systematic scale error during VLBI data reduction, is part of an ongoing effort.

Acknowledgments

The author wishes to thank R. N. Treuhaft and R. P. Linfield for their many valuable comments and critical reading of the manuscript. The author is also grateful to G. M. Resch for useful discussions.

References

[1] R. N. Treuhaft and G. E. Lanyi, "The Effect of the Dynamic Wet Troposphere on the Radio Interference Measurements," *Radio Science*, vol. 22, p. 251, 1987.

[2] R. N. Treuhaft and S. T. Lowe, "A Measurement of Planetary Relativistic Deflection," *The Astronomical Journal*, vol. 102, p. 1879, 1991.

[3] J. W. Armstrong, "Advanced Doppler Tracking Experiments," *Proc. of Workshop, NASA Conference on Relativistic Gravitational Experiments in Space*, Publication 3046, Annapolis, Maryland, June 28–30, 1988.

[4] G. M. Resch, "Inversion Algorithm for Water Vapor Radiometers Operating at 20.7 and 31.4 GHz," *TDA Progress Report 42-76*, vol. October–December 1982, Jet Propulsion Laboratory, Pasadena, California, pp. 12–26, February 15, 1983.

[5] A. J. Thompson, J. M. Moran, and G.W. Swenson, *Interferometry and Synthesis in Radio Astronomy*, New York: John Wiley and Sons, 1986.

[6] W. C. Hamilton, *Statistics in Physical Science*, New York: The Ronald Press, 1964.

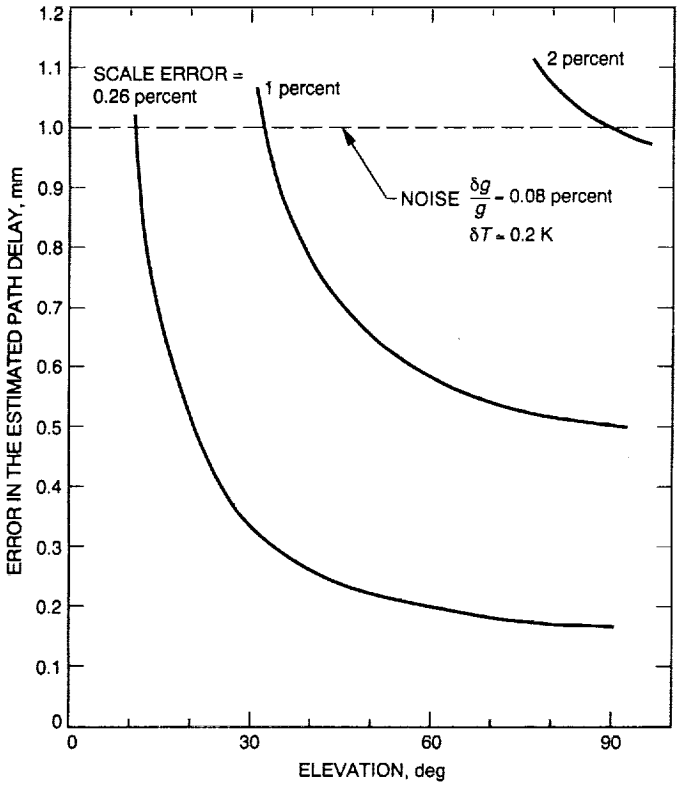

Fig. 1. The effect of stochastic (e.g., due to thermal noise and WVR gain variation) and scale (e.g., from absorption coefficient and WVR calibration) errors on path-delay estimates. The scale errors plotted are per 1 g/cm^2 of water vapor zenith column density (or, equivalently, per 6 cm of zenith path delay). The goal is 1-mm path-delay calibration accuracy in most weather conditions. (This figure assumes no reduction in the effects of a scale error from parameter estimation.)

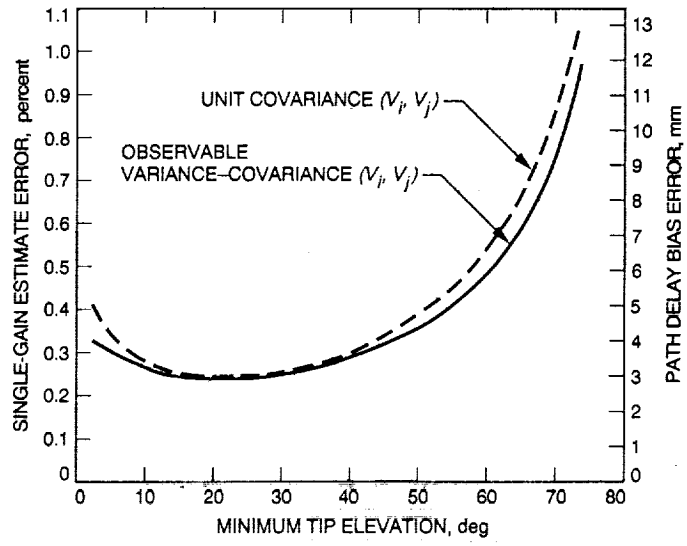

Fig. 2. The standard deviation of a single gain estimate from tip curves versus minimum tip elevation. The heavy and broken line curves were calculated using the actual and unit observable covariance–variance matrix W^{-1} in the least-squares analysis. The path delay shown is the bias error ΔL_V.

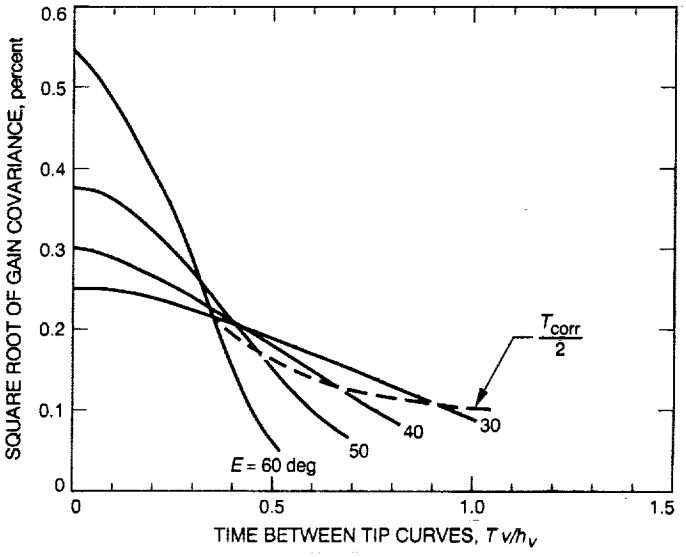

Fig. 3. Temporal development of the square root of the covariance of successive gain estimates versus time, T, elapsed between tip curves. The single gain estimates decorrelate within the time $T_{corr} = h_v/(v \tan E_{min})$. The broken line curve connects covariance values at $T = T_{corr}/2$.

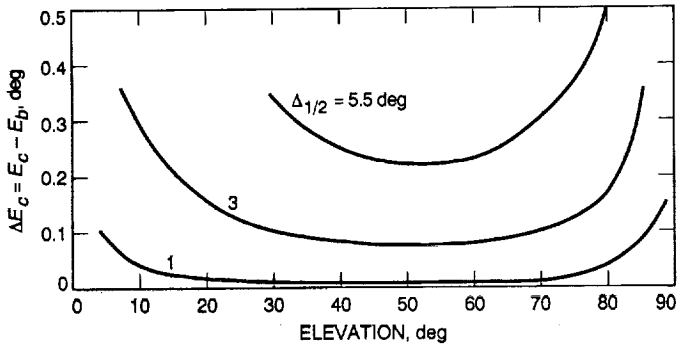

Fig. 4. The offset (ΔE_c) between elevations of the WVR beam geometrical center and brightness centroid. For small beam widths, $\Delta E_c \propto \Delta^2_{1/2}$. Note that as E_c approaches 90 deg, the offset increases to $\Delta_{1/2}/\sqrt{3}$.

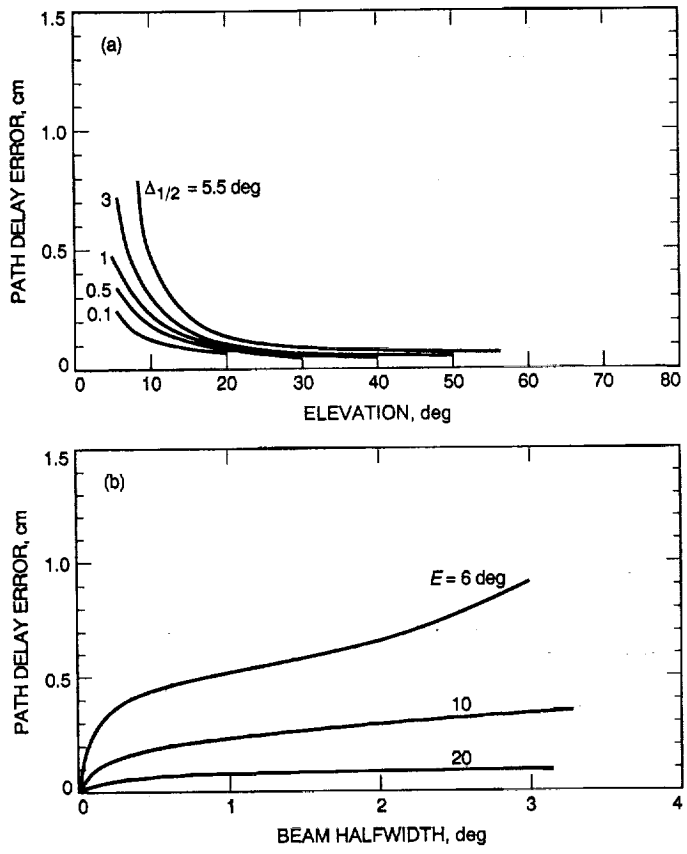

Fig. 5. Path delay stochastic error for the brightness centroid pointing due to WVR beam averaging of tropospheric fluctuations (instantaneous error, per 1 g/cm^2 of zenith water vapor column density): (a) versus elevation and (b) versus beam half-width.

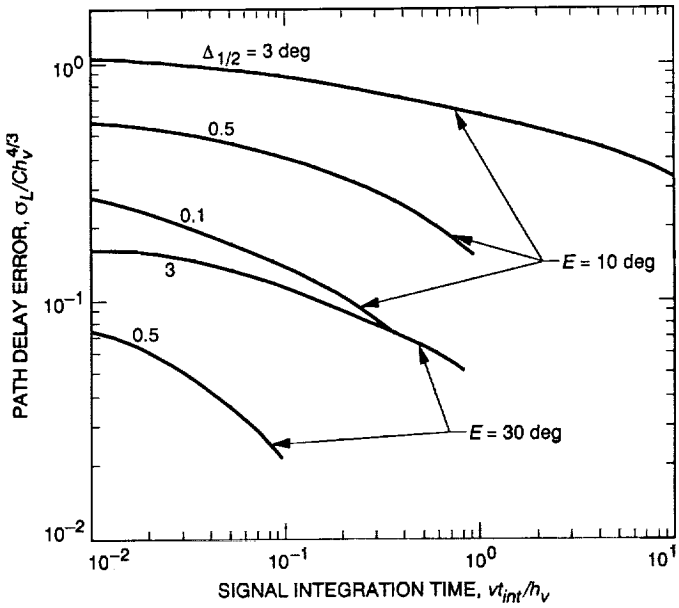

Fig. 6. Path delay stochastic error for the brightness centroid pointing versus the signal integration time. For a symmetrical radiation pattern, the error depends only very little on the wind direction (for different wind directions, the calculated errors differed by less than 15 percent).

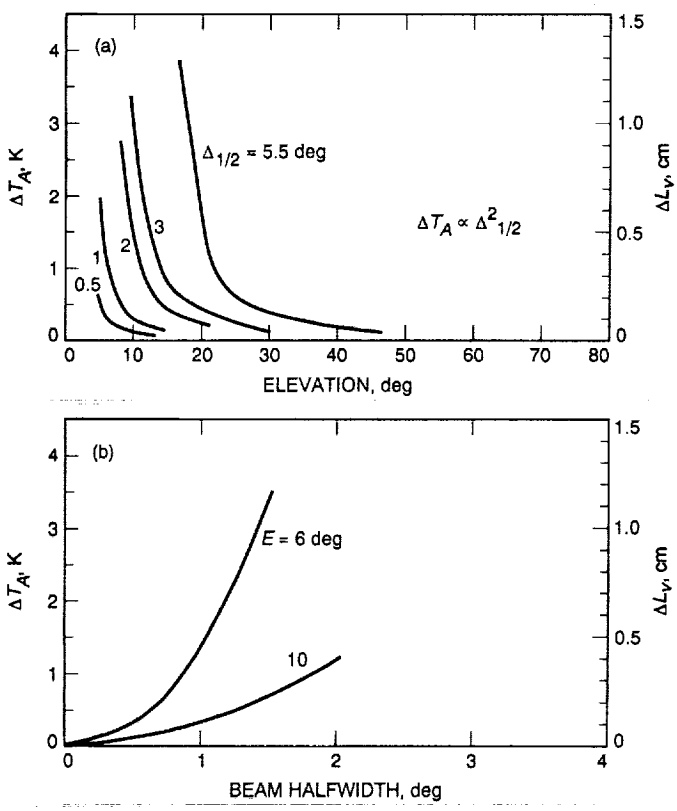

Fig. 7. The systematic difference ΔT_A between the antenna temperature and the brightness temperature at 20.6 GHz (and the corresponding path delay error) in the beam geometrical center due to WVR beam width averaging of air mass (per 1 g/cm^2 of zenith water vapor column density): (a) versus elevation and (b) versus beam half-width.

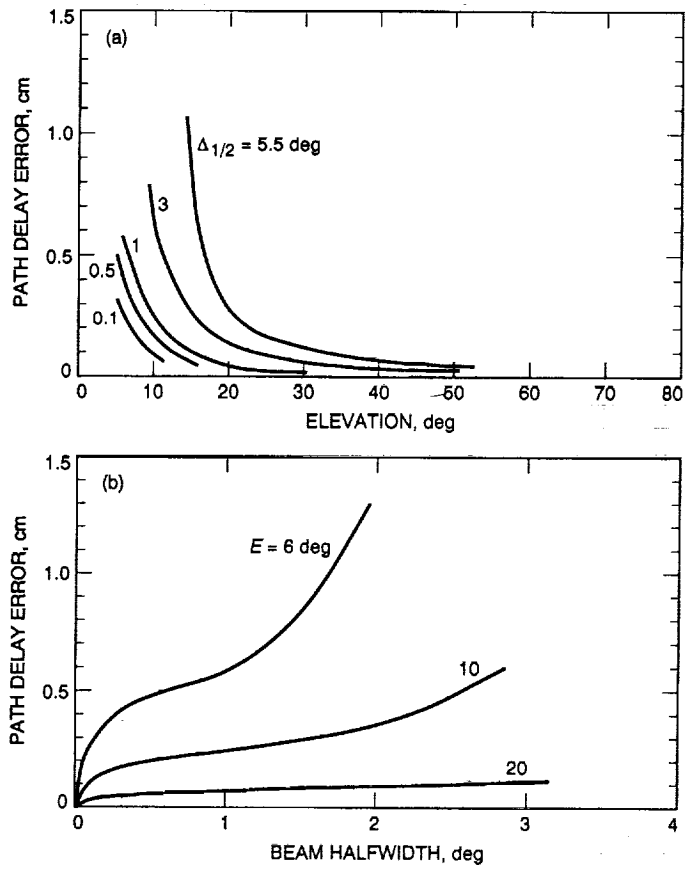

Fig. 8. Path delay stochastic error for the geometrical center pointing due to WVR beam averaging of tropospheric fluctuations (per 1 g/cm^2 of zenith water vapor column density): (a) versus elevation and (b) versus beam half-width.

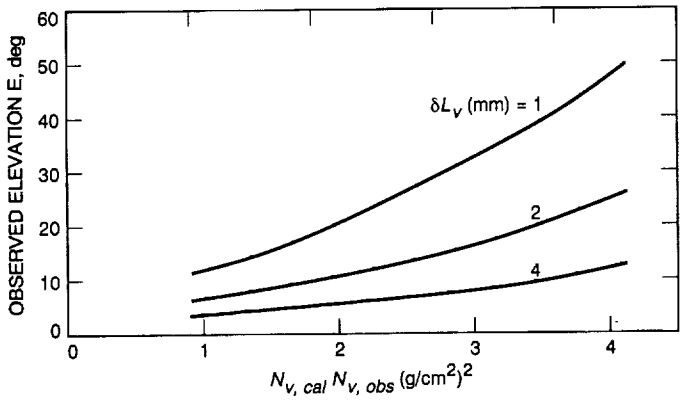

Fig. 9. Curves of path delay scale errors (δL_v) for a single gain estimate. For each curve, the error is less than the cutoff error above and to the left of the curve. The values of $N_{v,cal}$ and $N_{v,obs}$ are zenith water vapor column densities during WVR calibration and radiometric observation, respectively.

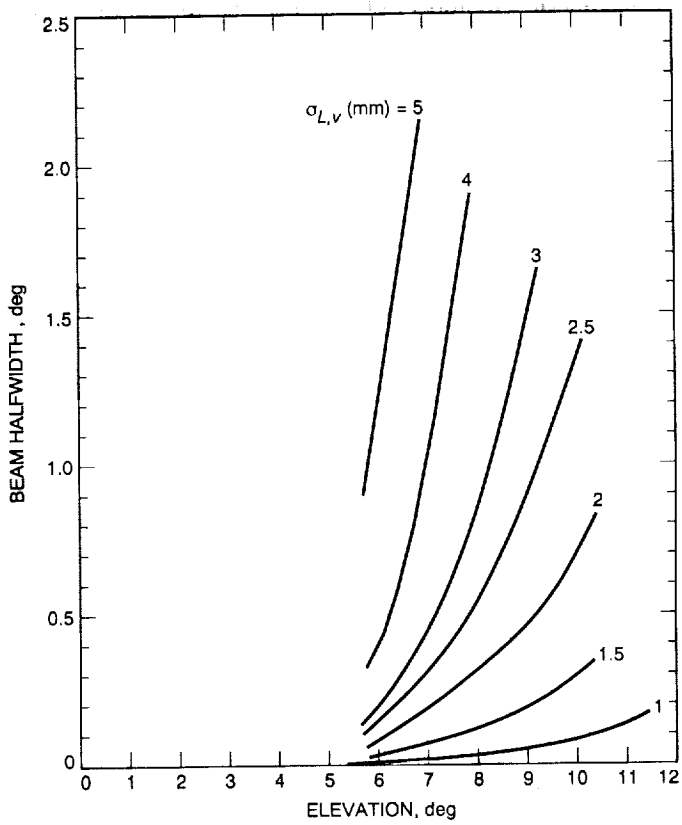

Fig. 10. Curves of tropospheric fluctuation-induced path delay error ($\sigma_{L,v}(E_b)$) for the brightness centroid (per 1 g/cm^2 of zenith water vapor column density) due to WVR beam averaging. In more humid weather, the errors scale with humidity.

Appendix A

The Method of Least Squares

For brevity of notation, the voltage recorded by a WVR pointed in a direction E_i is designated V_i, and the line-of-sight opacity is designated τ_i. The duration of a single tip sequence is less than the time it takes to decorrelate the tropospheric inhomogeneities. The ith tip curve voltage, V_i, is then modeled as

$$V_i = g\left(T_C\, e^{-\tau_i} - T_M(1 - e^{-\tau_i}) - T_{ref}\right)$$

$$\simeq g\,\tau_i\,T_{MC} - g\,T_{RC} \qquad \text{(A-1)}$$

where $T_{RC} = T_{ref} - T_C$, $T_{MC} = T_M - T_C$, and where the linearized Eq. (A-1) is a good approximation to the full radiation transport equation for most ($\tau_i < 0.5$) tropospheres of interest.

In tip curve analyses, the WVR recorded data are fit by assuming a temporally constant and spatially homogeneous stratified troposphere. For $i = 1, \ldots N$ data, where N is the number of tip curve elevations, the V_i's represent a set of N equations for two solve-for parameters, $\hat{g}$ and $\hat{\tau}_z$. Mapping the τ_i's to zenith by using $\tau_i = \hat{\tau}_z, A_i$, where $\hat{\tau}_z$ is the estimate for the zenith opacity τ_z, and the air mass $A_i = 1/\sin E_i$, the equations are solved by the method of least squares [6], as follows.

Defining solve-for parameters and observable column vectors $X = [g\ \tau_z,\ g]$ and $V = [V_1, \ldots V_N]$, respectively, the design matrix $\mathcal{A}$ ($\mathcal{A}$ has dimensions $N \times 2$) in $V = \mathcal{A}\,X$ is

$$\mathcal{A} = \begin{pmatrix} T_{MC}A_1 & -T_{RC} \\ T_{MC}A_2 & -T_{RC} \\ \vdots & \vdots \\ T_{MC}A_N & -T_{RC} \end{pmatrix} \qquad \text{(A-2)}$$

Assuming that the errors in V_i's have zero means and a variance–covariance matrix W^{-1}, minimization of the quadratic form $((V - \mathcal{A}\hat{X})^T\ W\ (V - \mathcal{A}\hat{X}))$ yields the following estimates for g and τ_z:

$$\hat{X} = (\mathcal{A}^T W \mathcal{A})^{-1}\mathcal{A}^T W\ V \qquad \text{(A-3)}$$

where $\hat{X}$ is the column vector $\hat{X} = [\,g\hat{\tau}_z,\ \hat{g}]$, and the superscript T designates the transpose matrix. By substituting Eq. (A-1) into Eq. (A-3), one can easily verify that the statistically averaged estimated gain is equal to the WVR gain (i.e., $\langle\hat{g}\rangle = g$), as it should be. The estimated gain standard deviation is the square root of $\sigma^2_{\hat{g}} \equiv \mathrm{cov}(\hat{g}, \hat{g})$, which is the matrix element $(\sigma^2_{\hat{X}})_{2,2}$ of

$$\sigma^2_{\hat{X}} \equiv Exp\ \{(\hat{X} - X)(\hat{X} - X)^T\}$$

$$= B^{-1}\mathcal{A}^T W\ \mathrm{cov}(V, V^T)\ W\ \mathcal{A}\ B^{-1} \qquad \text{(A-4)}$$

where Exp designates the expectation value, $\mathrm{cov}(V, V^T)$ is the actual observable covariance–variance matrix, and $B = \mathcal{A}^T W \mathcal{A}$. Equations (A-3) and (A-4) yield $\hat{g}$, $\hat{\tau}_z$, and $\sigma^2_{\hat{X}}$ for given W_{ij} and $\mathrm{cov}(V, V^T)$.

In practice, $\hat{X}$ and $\sigma^2_{\hat{X}}$ can be derived either by using some assumed W^{-1} (the so-called consider analysis) [1], or by setting W^{-1} equal to the observable variance–covariance matrix $\mathrm{cov}(V, V^T)$. The most common (and simplest) form of the assumed W^{-1} is the unit matrix $(W^{-1})_{i,j} = \delta_{i,j}$, where $\delta_{i,j}$ is the Kronecker delta. Taking the unit W^{-1} corresponds to assuming that the observable errors are uncorrelated with equal variances and reduces the minimization procedure to the minimization of the sum of squares. The latter, i.e., setting $(W^{-1})_{i,j} = \mathrm{cov}(V_i, V_j)$, minimizes the variance–covariance matrix $\sigma^2_{\hat{X}}$ as $\sigma^2_{\hat{X}} = (\mathcal{A}^T W \mathcal{A})^{-1}$.

The results of these calculations are discussed in the main text. Evaluation of $\mathrm{cov}(V_i, V_j)$ using the Kolmogorov turbulence model is described in Appendix B.

Appendix B

Evaluation of the Correlation Functions Using the Kolmogorov Turbulence Model

To evaluate correlations between the simulated data, the voltage V_i associated with the sky brightness $T_{B,i}$ in the elevation direction E_i is first related to the line-of-sight opacity τ_i by using Eq. (A-1). This expresses correlations between V_i's in terms of correlations between τ_i's. Next, neglecting fluctuations in the dry component of τ_i, correlations between wet opacities are expressed in terms of correlations of wet refractivity by expressing the wet opacity ($\tau_{v,i}$) as the line-of-sight integral

$$\tau_{v,i} = \int_0^{h_v/\sin E_i} \alpha_v(\vec{r}_i)\, dr_i \simeq \frac{\tau_{v,z}}{L_{v,z}} \int_0^{h_v/\sin E_i} \chi(\vec{r}_i) dr_i \tag{B-1}$$

where h_v is the height of the tropospheric slab; α_v is the water vapor absorptivity per unit length; $\tau_{v,z}$ and $L_{v,z}$ are the average values of wet opacity and path delay at zenith, respectively; and $\chi(\vec{r}_i)$ is the index of refraction − 1. The correlations between $\chi(\vec{r}_i)$'s are evaluated by using the Kolmogorov turbulence structure function, Eq. (8) of the main text. In what follows, the above described procedure of evaluating the correlations is exemplified in the evaluation of the observable variance–covariance matrix W^{-1}.

By using Eq. (A-1), the matrix element $W_{i,j}^{-1}$ is written as

$$W_{i,j}^{-1} \equiv \mathrm{cov}(V_i, V_j) = g^2 T_{MC}^2\, \mathrm{cov}(\tau_{v,i}, \tau_{v,j})$$

$$= g^2 T_{MC}^2 \left(\langle \tau_{v,i}, \tau_{v,j}\rangle - \langle \tau_{v,i}\rangle \langle \tau_{v,j}\rangle\right) \tag{B-2}$$

where $\langle ... \rangle$ signifies statistical ensemble averaging.

By using Eq. (B-1) and the expression (Eq. A.3 of [1])

$$\langle \chi_i \chi_j \rangle = \langle \chi^2 \rangle - \frac{1}{2} D_\chi(\vec{r}_i - \vec{r}_j) \tag{B-3}$$

where $\chi_i \equiv \chi(\vec{r}_i)$ and $D_\chi(\vec{r}_i - \vec{r}_j) \equiv \langle (\chi_i - \chi_j)^2 \rangle$ is the refractivity spatial structure function by interchanging the order of integration and ensemble averaging, and then setting $dr_i = A_i\, dz$ and $dr_j = A_j\, dz'$, Eq. (B-2) yields

$$W_{ij}^{-1} = \left(\frac{\tau_{v,z}\, g\, T_{MC}}{L_{v,z}}\right)^2 A_i A_j$$

$$\times \int_0^{h_v} dz \int_0^{h_v} dz' \left(\sigma_\chi^2 - \frac{D_\chi(\vec{r}_i - \vec{r}_j)}{2}\right) \tag{B-4}$$

where the variance σ_χ^2 of the wet refractivity fluctuation is independent of spatial coordinates and is obtained by letting the distance R go to infinity in

$$\sigma_\chi^2 \equiv \left(\langle \chi^2 \rangle - \langle \chi \rangle^2\right) = \frac{D_\chi(R=\infty)}{2} = \frac{N_v^2\, C^2\, L_s^{2/3}}{2} \tag{B-5}$$

where the last expression on the right-hand side has been obtained by evaluating the asymptotic $D_\chi(R=\infty)$ by using Eq. (8) of the main text, and where N_v is the water vapor column density at zenith in g/cm^2, and L_s is the tropospheric turbulence saturation length. The reason why $D_\chi(\infty)$ should converge as R becomes very large has been discussed in [1].

The covariance of successive gain estimates and the effect of signal integration on beam averaging of tropospheric fluctuations involve evaluation of correlations of type $\langle \tau_i(t)\tau_j(t+T)\rangle$. By using the "frozen" troposphere model [1], these correlations were evaluated using the expression

$$\langle \chi(\vec{r}_i, t)\chi(\vec{r}_j, t+T)\rangle = \langle \chi^2 \rangle - \frac{1}{2} D_\chi(\vec{r}_i - \vec{r}_j + \vec{v}\,T) \tag{B-6}$$

where the structure function

$$D_\chi(\vec{r}_i - \vec{r}_j + \vec{v}\,T) = \left\langle \left(\chi(\vec{r}_i, t) - \chi(\vec{r}_j, t+T)\right)^2 \right\rangle$$

is the same as Eq. (8) of the main text.